International Journal of Science and Research (IJSR)
ISSN (Online): 2319-7064
Index Copernicus Value (2016): 79.57 | Impact Factor (2017): 7.296

Vibrational Spectral Analysis, HOMO-LUMO plot and Electrostatic Potential Surface Map of Dimethylisophthalate

R. Gopala Krishnamani[1], V. Balachandran[2]

[1]Department of Physics, Seshasayee Institute of Technology, Tiruchirappalli -620 010, India

[2]Centre for Research-Department of Physics, Arignar Anna Government Arts College, Musiri, Tiruchirappalli – 621 211, India

Abstract: ***The FT-IR and FT-Raman spectra of dimethylisophthalate have been recorded in the region 4000-400 cm^{-1} and 3500-100 cm^{-1} respectively. Optimized geometrical structure and harmonic vibrational frequencies have been computed by the B3LYP density functional levels using 6-31G(d,p) and 6-311++G(d,p) basis sets. The observed FT-IR and FT-Raman vibrational frequencies are analyzed. The geometries and normal modes of vibration obtained from DFT method are in good agreement with the experimental data. The charge transfer occurring in the molecule between HOMO and LUMO energies, frontier energy gap, the molecular electrostatic potential have been were calculated and analyzed.***

Keywords: Vibrational spectra, HOMO-LUMO, MEP, dimethylisophthalate

1. Introduction

One of the principal uses of dimethyl isophthate (DMP) is an intermediate in the synthesis of polyesters. In order to obtain the structural strength needed in fibers and films the polyesters must be of high molecular weights is through transesterification of methyl ester with a glycol. A specially purified methyl ester is needed in this application. It is used primarily to improve the clarity and strength of carbonated drink bottles. Another signification area is in engineering plastics. Molecular structures of phthalate, isophthalate and tereph-thalate acids were described in the works of Nowacki and Jaggi [1] Derissen [2] and Bailey and Brown [3]. Conformational studies of methyl-terephthalate were carried out by Brisse and Pérez [4]. Fourier transform infrared and Raman spectra. Semi empirical ab initio calculations for dimethylterephthalate were analyzed by Téllez et al [5]. Wang et al [6] have been studied the FT-IR, Raman and NMR spectra, molecular geometry, vibrational assignments for diethyl phthalate.

Literature survey reveals that to the best of our knowledge, the results based on quantum chemical calculations. FT-IR and FT-Raman spectral studies on DMP have no reports. Hence in the present work, we reported detailed interpretations of the infrared and Raman spectra based on the experimental and theoretical results, which are acceptable and supportable to each other. Attempts have been made to find out an optimum method using a reasonable basis set to get a close agreement between the computed and experimental data.

2. Methodology

The compound DMP was purchased from Lancaster chemical company, UK, with a stated purity of 98% and it was used as such without further purification. The spectral measurements were carried out at central Electrochemical Research Institute (CECRI), Karaikudi (Tamilnadu) India. The FT-Raman spectrum of DMP was recorded using 1064 nm line of Nd: YAG laser as excitation wavelength in the region 3500-100 cm^{-1} on thermo electron corporation module accessory. FT-IR spectral measurements were carried out at St. Joseph College, Tiruchirappalli, India. The FT-IR spectrum of the title compound was recorded in the region 4000-400 cm^{-1} on Perkin Elmer spectrophotometer. The spectrum was recorded at room temperature with a scanning speed of 30 cm^{-1} min^{-1} and the spectral width of 2.0 cm^{-1}. The observed experimental FT-IR and FT-Raman spectra and shown in Figs. 1 and 2, respectively.

3. Computational Method

Geometry optimization and vibrational frequencies of dimethyl isophthalate were calculated at the B3LYP (Beecke-3-Lee-Yang-Parr three parameters)hybrid functional with correlation function such one proposed by Lee, Yang and Parr [7] (B3LYP) is most promising in providing reasonably acceptance vibrational wave numbers for organic molecules, Statements 6-311++G(d,p) basis set has been used in both methods in order to see the effect of correlation. Gaussian 09 software [8] package and the methods implemented therein have been utilized to accomplish all the calculation. All the parameters were allowed to relax and all the calculations were converged to an optimized Geometry which corresponds to imaginary values in the wave numbers calculations. The Cartesian representation of the theoretical force constants have been computed at the fully optimized geometry by assuming the molecule belongs to Cs point group symmetry. The transformation of force field from Cartesian to internal local symmetry co-ordinate analysis(NCA), calculation of potential energy distribution(PED) were done on a pc with the version V7.0-G77 of MOLVIB program written by Tom Sundius [9].

4. Result and Discussion

4.1 Geometric structure

The title molecule belongs to Cs point group symmetry. The optimized structural parameters (Table 1) of DMP were calculated by B3LYP/6-31G(d,p)and B3LYP/6-311++G(d,p) levels. In accordance with the atom numbering scheme is given in Fig.1. The global minimum energies of DMP are -688.022240557 hartrees and -688.204392948 hartrees by B3LYP/6(d,p) and B3LYP/6(d,p) levels, respectively. The computed harmonics were scaled by 0.8901 for wave numbers.

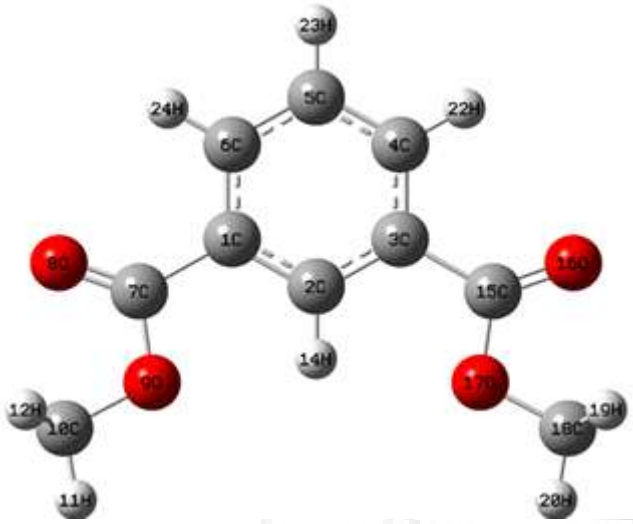

Figure 1: Optimized molecular structure of dimethylisophthalate

4.2 Vibrational assignments

The 66 normal modes of DMP are distributed among the symmetry species as $\sqrt{3}$N-3=45 A' (in-plane) +21 A" (out-of-plane) by assuming Cs point group symmetry. The detailed vibrational assignments of fundamental modes of DMP along with observed and calculated frequencies and normal mode descriptions are listed in Table 2. The recorded FT-IR and FT-Raman spectra of the title compound are shown in Figs. 2 and 3, respectively. It is contentment to discuss the vibrational spectra of DMP in term of the characteristic spectral region as described below:

C-H vibrations

The heteroaromatic organic compounds commonly exhibit multiple week bands in the region 3100-3000 cm^{-1} due to C-H stretching vibrations [10]. In this region, the bands are not affected appreciably by the nature of substituents. In this title molecule, the bands have been assigned at 3095 cm^{-1} in IR and 3110, 3094, 3080 cm^{-1} in Raman to C-H stretching vibrations. The scaled values computed by B3LYP/6-311++G(d, p) level coincide well with the experimental observation. The C-H in-plane ring bending vibrations normally occurred as a number of strong to weak intensity sharp bands in the region 1300-1000 cm^{-1}. The bands for C-H in-plane bending vibrations of the compound identified at 1314 and 1293 cm^{-1} infrared and 1315 cm^{-1} in Raman. The theoretically computed frequency for C-H in-plane bending vibrations by B3LYP/6-311++G(d, p) method shows agreement with recorded spectra as well as literature data [10].

The C-H out-of-plane bending vibrations are strongly coupled vibrations and normally observed in the region 1150-800 cm^{-1}. In the present case, the bands are identified at 1174 and 998 cm^{-1} for C-H out-of-plane bending.

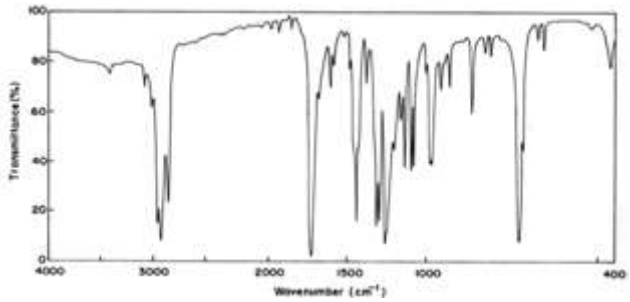

Figure 2: Observed FTIR spectrum of dimethylisophthalate

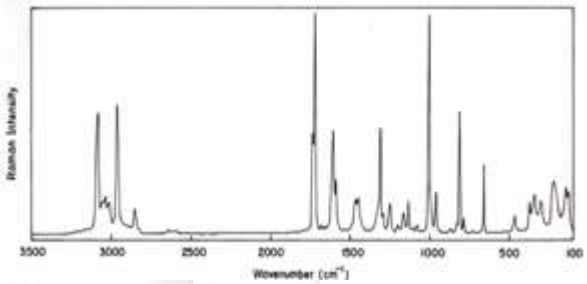

Figure 3: Observed FT-Raman spectrum of dimethylisophthalate

C-O and C=O vibrations

The C-O stretching vibration in DMP has the main contribution in the mode with B3LYP/6-31G(d, p) and B3LYP/6-311++G(d, p) predicted frequencies at 1806, 1800, 1510, 1343, 1272, 1221 and at 1771, 1765, 1497, 1321, 1249, 1214 cm^{-1} (Table 4.3). The computed wavenumber obtained by B3LYP/6-311++G(d, p) are in agreement with very strong experimental frequencies at 1720, 1490, 1260, 1200 cm^{-1} in IR and at 1735, 1305, 1206, 1200 cm^{-1} in FT Raman spectrum. The in-plane and out-of-plane C-O bending vibration mode with the theoretical frequency is found to be in agreement with the calculated values of B3LYP/6-311++G(d, p) level with basis set. The above conclusion is in agreement with literature value [11].

CH_3 vibrations

The O-CH_3 stretching and bending modes appear to be quite pure group vibrations. Considering the assignment of CH_3 group frequencies, one can expect that nine fundamentals and can be associated to each CH_3 group, namely the symmetrical $\nu_s(CH_3)$, and asymmetrical $\nu_a(CH_3)$, in-plane stretching modes; the symmetrical $\delta_s(CH_3)$ and asymmetrical $\delta_a(CH_3)$, deformation modes; the in-plane rocking and out-of-plane rocking and twisting bending modes. The asymmetric stretching and asymmetric deformation modes of the methyl group are expected to be depolarised for A″ symmetry species. The FT-IR band found at 2925 and 2900 cm^{-1} is assigned to $\nu_s(CH_3)$. The infrared bands observed at 3012, 3000 and 2955 cm^{-1} were due to asymmetric stretching vibrations of the methyl group. The two in-plane methyl

deformation modes were also well established. The band observed at 1462 cm^{-1} in Raman was attributed to asymmetric deformation of the methyl group. The symmetrical methyl deformation mode was found at 1474 cm^{-1} in Raman and 1450 cm^{-1} in IR spectra. The medium strong infrared and very strong Raman bands found at 1092 cm^{-1} was due to out-of-plane symmetric deformation of the methyl group. The CH_3 deformational modes mainly coupled with the in-plane bending vibrations. The bands obtained at 980, 965 cm^{-1} and 946, 879 cm^{-1} in IR were assigned to in-plane and out-of-plane rocking modes

C-C vibrations

The ring carbon-carbon stretching vibrations occur in the region 1625-1430cm^{-1}. The in-plane-deformation vibration is at higher frequencies than the out-of-plane vibrations. In the present work, the frequencies observed in the FT-Raman spectrum at 1618 cm^{-1} has been assigned to C-C stretching vibration. The theoretically computed values by B3LYP/6-311++G(d, p) methods for C-C vibrations are agreement with experimental values.

4.3 HOMO, LUMO analysis

The most important orbitals in the molecule are the frontier molecular orbitals, called highest occupied molecular orbital (HOMO) and lowest unoccupied molecular orbital (LUMO). These orbitals determine the way of molecule interacts with other species. The frontier molecular energy gap helps to characterize the chemical reactivity and kinetic stability of the molecule. A molecule with a small frontier orbital gap is more polarizable and is generally associated with a high chemical reactivity, low kinetic stability and is also termed as soft molecule [60]. The low values of the frontier orbital gap in DMP make it more chemically reactive and less kinetic stable. The conjugated molecules are characterized by a small highest occupied molecular orbital-lowest unoccupied molecular orbital (HOMO–LUMO) separation, which is the result of a significant degree of intramolecular charge transfer from the end-capping electron acceptor groups through p-conjugated path [61]. The 3D plot of the frontier orbital's HOMO and LUMO of DMP molecule is shown in Fig. 4.

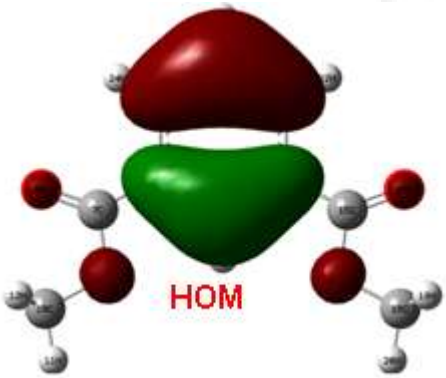

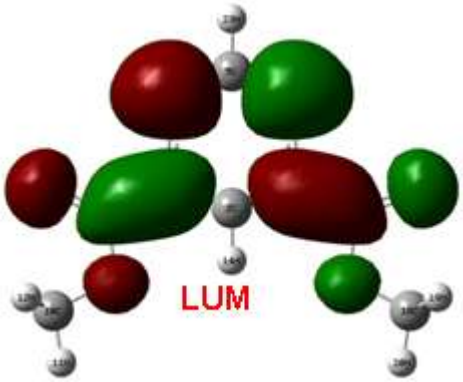

Figure 4: HOMO-LUMO plot of dimethylisophthalate

The positive phase is red and negative phase one is green. Many organic molecules, conjugated p electrons are characterized by large values of molecular first hyperpolarizabilities, were analyzed by means of vibrational spectroscopy [62, 63]. In most cases, even in the absence of inversion symmetry, the strongest band in the FT-Raman spectrum is weak in the FT-IR spectrum vice versa. But the intramolecular charge transfer from the donor-acceptor group in a single-double bond conjugated path can induce large variations of both the dipole moment and the polarizability, making FTIR and FT-Raman activity strong at the same time. This electronic transition absorption corresponds to the transition from the ground to the first excited state and is mainly described by an electron excitation from the HOMO to LUMO. An electron excitation from the highest occupied molecular orbital to the lowest unoccupied molecular orbital (HOMO–LUMO).

4.4 Molecular electrostatic potentials

Molecular electrostatic potential (MEP) at a point in the space around a molecule gives an indication of the net electrostatic effect produced at that point by the total charge distribution (electron + nuclei) of the molecule and correlates with dipole moments, electronegativity, partial charges and chemical reactivity of the molecule. It provides a visual method to understand the relative polarity of the molecule. An electron density isosurface mapped with electrostatic potential surface depicts the size, shapes, charge density and site of chemical reactivity of the molecules. Such mapped electrostatic potential surface has been plotted for the title molecule B3LYP/6-311++G(d, p) basis set using the computer software Gauss view [30]. A Projection of this surface along the molecular plane is given Fig 5.

The different values of the electrostatic potential at the surface are represented by a different color: red represents the regions of the most negative electrostatic potential, blue represents the regions of the most positive electrostatic potential, and green represents the regions of zero potential. Electrostatic potential decreases in the order red < orange < yellow < green < blue. In all causes; the shapes of the electrostatic potential surface is influenced by the structure and charge density distributions in the molecule with sites close to the oxygen atom, showing region of most negative electrostatic potential. This Fig. 5 provides a visual representation of the chemically active sites and comparative

reactivity of atoms. It may see that, a region of zero potential envelopes the π system of the aromatic rings, leaving a more electrophilic region in the plane of hydrogen atoms in title molecule.

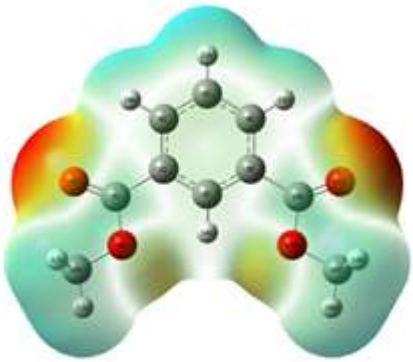

Figure 5: MEP surface map of dimethylisophthalate

5. Conclusion

The optimized molecular parameters such as bond length and bond angles of dimethyl isophthalate were calculated DFT/B3LYP/6-31G(d,p)/6-311++G(d,p) levels of theory. The harmonic-vibrational frequencies dimethyl isophthalate have also been determined and analyzed both at the basis sets. The difference between the corresponding wave numbers (observed and calculated) is very small, for most of the fundamentals. The theoretically computed wave numbers of dimethyl isophthalate by DFT/B3LYP/6-311++G(d,p) method shows good agreement with experimental results. Therefore, the results presented in this work for dimethyl isophthalate indicates that this level of theories reliable for prediction of both infrared and Raman spectra of the title compound.

References

[1] W. Nowacki, H. Jaggi, Z. Kristallogr. 109 (1957) 272.
[2] J.L. Derissen, Acta Cryst. B-30 (1974) 2764; R.W.G. Wyckoff, Crys-tal Structures, second ed., vol. 6, Part 1, Interscience Publishers, New York, 1969, p. 178–181.
[3] M. Bailey, C.J. Brown, Acta Cryst. 22 (1967) 387.
[4] F. Brisse, S. Pérez, Acta Cryst. B-32 (1976) 2110.
[5] Claudio A. Téllez S, Eduardo Hollauer, Tiago Giannerini, M.I. Pais da Silva, M.A. Mondragón, J.R. Rodr´ıguez T, V.M. Castaño, Spectrochimica Acta Part A 60 (2004) 2171–2180.
[6] M. Wang, J.J. Geng, Z.B. Wei, Z.Y. Wang, Jiegou Hauxue, 32 (2013) 890-902.
[7] C. Lee, W. Yang, R.C. Parr, J. Phys. Rev. B 37 (1998) 785–789.
[8] M.J. Frisch, G.W. Trucks, H.B. Schlegel, G.E. Scuseria, M.A. Robb, J.R.Cheeseman, V.G. Zakrzewski, J.A. Montgomery, Jr., R.E. Stratmann, J.C. Burant, S. Dapprich, J.M. Millam, A.D. Daniels, K.N. Kudin, M.C. Strain, O. Farkas, J. Tomasi, V. Barone, M. Cossi, R. Cammi, B. Mennucci, C. Pomelli, C. Adamo, S. Clifford, J. Ochterski, G.A. Petersson, P.Y. Ayala, Q. Cui, K. Morokuma, N. Rega, P. Salvador, J.J. Dannenberg, D.K. Malick, A.D. Rabuck, K.Rahavachari, J.B. Foresman, J. Cioslowski, J.V. Ortiz, A.G. Baboul, B.B. Stefanov, G. Liu, A. Liashenko, P. Piskorz, I. Komaromi, R. Gomperts, R.L. Martin, D.J. Fox, T. Keith, M.A. Abraham, C.Y. Peng, A. Nanayakkara, M. Challacombe, P. Gill, B. Johnson, W. Chen, M.W. Wong, J.L. Andres, C. Gonzalez, M. Head Gordon, E.S. Replogle, J.A. Pople, Gaussian09, Revision A11.4, Gaussian Inc., Pittsburgh, PA, 2008.
[9] (a)T. Sundius, J. Vib. Spectrosc. 29 (2002) 89–95. b)MOLVIB: A program for Harmonic Force Field Calculations, QCPE Program No. 807. 2002.
[10] G.Socrates, Infrared and Raman Characteristic Group Frequencies - Tables and Charts, third ed., Wiley, Chichester, 2001.
[11] R.M. Silverstein, G. Clayton Bassler, Erence C. Morrill, Spectrometric Identification of Organic Compounds, Fifth ed., John Wiley & Sons, Inc, New York.
[12] B.J. Powell, T.Baruah, N. Bernstein, K. Brake, R.H.McKenzie, P. Meredith, M.R. Pederson, J. Chem. Phys.2004;120;8608–8615.
[13] C.H. Choi, M. Kertesz, J. Phys. Chem.1997;A101;3823–3831.
[14] Y. Ataly, D. Avci, A. Basoglu, J. Struct. Chem. 2008;19 ;239–246.
[15] T. Vijayakumar, I. Hubert Joe, C.P.R Nai V.S. Jayakumar, J. Chem.Phys. 2008;343; 83–99.
[16] M.J. Frisch, A.B. Nielsm, A.J. Holder Gaussview User Manual, Gaussian Pitsburgh, 2008.

Table 1: Optimized geometrical parameters of dimethyl isophthalate based on B3LYP level with 6-31G(d,p) and 6-311++G(d,p) basis sets.

Parameters	6-31G (d,p)	6-311++ G(d,p)	Parameters	6-31G (d,p)	6-311++ G(d,p)
C_1-C_2	1.40	1.40	C_2-C_1-c_6	119.96	119.89
C_1-C_6	1.40	1.40	C_2-C_1-c_7	122.33	122.19
C_1-C_7	1.49	1.49	C_6-C_1-C_7	117.71	117.92
C_2-C_3	1.40	1.40	C_1-C_2-C_3	119.77	119.89
C_2-H_{14}	1.08	1.08	C_1-C_2-H_{14}	120.12	120.05
C_3-C_4	1.40	1.40	C_3-C_2-H_{14}	120.11	120.05
C_3-C_{15}	1.49	1.49	C_2-C_3-C_4	119.95	119.89
C_4-C_5	1.39	1.39	C_2-C_3-C_{15}	122.34	122.19
C_4-H_{22}	1.08	1.08	C_4-C_3-C_{15}	117.70	117.92
C_5-C_6	1.39	1.39	C_3-C_4-H_{22}	120.20	120.15
C_5- H_{23}	1.09	1.08	C_3-C_4-H_{22}	118.42	118.68
C_6-H_{24}	1.08	1.08	C_5-C_4-H_{22}	121.38	121.17
C_7-O_8	1.22	1.21	C_4-C_5-C_6	119.93	120.03
C_7-O_9	1.35	1.35	C_4-C_5-H_{23}	120.03	119.99
O_9-C_{10}	1.44	1.44	C_6-C_5-H_{23}	120.03	119.99
C_{10}-H_{11}	1.09	1.09	C_1-C_6-C_5	120.19	120.15
C_{10}-H_{12}	1.09	1.09	C_1-C_6-H_{24}	118.42	118.68
C_{10}-H_{13}	1.09	1.09	C_1-C_7-O_8	121.39	121.17
CI_5-O_{16}	1.22	1.21	C_1-C_7-O_9	124.36	124.33
C_{15}-O_{17}	1.35	1.35	O_8-C_7-O_9	112.47	112.51
C_{17}-C_{18}	1.44	1.44	C_7-O_9-C_{10}	123.17	123.16
C_{18}-H_{19}	1.09	1.09	C_7-O_9-C_{10}	115.19	115.92
C_{18}-H_{20}	1.09	1.09	O_9-C_{10}-H_{11}	105.61	105.42
C_{18}-H_{21}	1.09	1.09	O_9-C_{10}-H_{12}	110.62	110.42
			O_9-C_{10}-H_{13}	110.62	110.42
			A_{11}-C_{10}-A_{12}	110.61	110.68
			H_{11}-C_{10}-H_{13}	110.61	110.68
			H_{12}-C10-H_{13}	108.76	109.18
			C^3-C_{15}-O_{16}	124.36	124.33
			C_3-C_{15}-O_{17}	112.46	112.51
			O_{16}-C_{15}-O_{17}	123.18	123.16
			C_{15}-O_{17}-C_{18}	115.22	115.90
			O_{17}-C_{18}-H_{19}	110.61	110.42
			O_{17}-C_{18}-H_{20}	105.61	105.42

			H_{19}-C_{18}-H_{20}	110.61	110.42
			H_{19}-C_{18}-H_{20}	110.61	110.68

			H_{19}-C_{18}-H_{21}	108.77	109.18
			H_{20}-C_{18}-H_{21}	110.61	110.68

Table 2: Optimized geometrical parameters of dimethylisophthalate based on B3LYP level with 6-31G(d,p) and 6-311++G(d,p) basis sets.

No.	Spe.	Observed frequency(cm^{-1})		Calculated frequency(cm^{-1})		Assignments / TED(%)
		FT-IR	Raman	6-31G(d,p)	6-311++G(d,p)	
1.	A'		3110 m	3254	3235	CH stretching(99)
2.	A'	3095 m	3094 s	3225	3205	CH stretching(98)
3.	A'		3080 s	3221	3200	CH stretching(98)
4.	A'		3016 m	3198	3280	CH stretching(99)
5.	A'	3012 w		3174	3157	CH_3 in-plane stretching(97)
6.	A'	3000 w	2975 s	3174	3157	CH_3 in-plane stretching(97)
7.	A''			3142	3124	CH_3 asymmetric stretching(98)
8.	A''	2955 m		3141	3124	CH_3 asymmetric stretching(97)
9.	A'	2925 ms		3064	3051	CH_3 symmetric stretching(95)
10.	A'	2900 m		3064	3051	CH_3 symmetric stretching(95)
11.	A'		1735 vw	1806	1771	CO stretching(92)
12.	A'	1720 m		1800	1765	CO stretching(92)
13.	A'			1656	1640	CC stretching(93)
14.	A'		1618 ms	1641	1625	CC stretching(94)
15.	A'			1525	1513	CH in-plane bending(88)
16.	A'			1510	1498	CH in-plane bending(86)
17.	A'	1490 w		1510	1497	CO stretching(85)
18.	A'		1474 vw	1496	1483	CH_3 in-plane bending(88)
19.	A'	1450 w		1495	1482	CH_3 in-plane bending(88)
20.	A''		1462 w	1484	1472	CH_3 out-of-plane bending(87)
21.	A''			1482	1471	CH_3 out-of-plane bending(89)
22.	A'		1374 w	1465	1453	CC stretching(89)
23.	A'	1314 s	1315 m	1373	1354	CH in-plane bending(84)
24.	A'		1305 ms	1343	1321	CO stretching(92)
25.	A'	1293 s		1326	1320	CH in-plane bending(82)
26.	A'	1260 m	1206 w	1272	1249	CO stretching(88)
27.	A'	1200 w	1200 w	1221	1214	CO stretching(87)
28.	A'			1216	1210	CC stretching(82)
29.	A''	1174 ms	1174 w	1190	1187	CH out-of-plane bending(66)
30.	A''		1156 w	1180	1172	CH out-of-plane bending(65)
31.	A'	1140 m		1180	1172	CC stretching(89)
32.	A'			1166	1154	Ring in-plane bending(72)
33.	A'	1112 s		1124	1113	Ring in-plane bending(72)
34.	A'		1092 w	1112	1105	CH_3 symmetric bending(66)
35.	A'	1012 w		1019	1017	CH_3 symmetric bending(69)
36.	A''		1000 vs	1018	1016	CH out-of-plane bending(59)
37.	A''	998 m	998 m	1013	1000	CH out-of-plane bending(58)
38.	A'	980 m	980 m	1000	982	CH_3 in-plane rocking(66)
39.	A'	965 m		980	978	CH_3 in-plane rocking(64)
40.	A''	946 ms		954	964	CH_3 out-of-plane rocking(58)
41.	A''		879 w	896	890	CH_3 out-of-plane rocking(58)
42.	A'	835 w		846	846	CO in-plane bending(64)
43.	A'	810 m		820	818	CO in-plane bending(65)
44.	A'	776 w		782	799	CC stretching(70)
45.	A'	734 s		736	746	CC stretching(72)
46.	A'	728 m		730	730	Ring in-plane bending(71)
47.	A'	674 m	675 ms	684	676	CC stretching(82)
48.	A'	662 m		670	670	CO in-plane bending(63)
49.	A'			532	531	CO in-plane bending(63)
50.	A'		473 w	481	476	CO in-plane bending(65)
51.	A''		410 vw	448	446	CO out-of-plane bending(55)
52.	A'		400 w	435	431	CO in-plane bending(62)
53.	A'		355 w	366	364	CO in-plane bending(62)
54.	A''		300 w	340	338	CO out-of-plane bending(58)
55.	A'			337	335	CC in-plane bending(67)
56.	A''			304	302	CO out-of-plane bending(58)
57.	A''		205 m	223	217	CO out-of-plane bending(54)
58.	A'			204	204	CC in-plane bending(63)

59.	A''		154 w	186	185	CO out-of-plane bending(52)
60.	A''		135 w	135	137	CO out-of-plane bending(55)
61.	A''			125	126	Ring out-of-plane bending(52)
62.	A''			114	111	CC out-of-plane bending(52)
63.	A''			99	97	CC out-of-plane bending(51)
64.	A''			91	91	Ring out-of-plane bending(45)
65.	A''			57	52	CH_3 torsion(48)
66.	A''			41	37	CH_3 torsion(48)